



MHD Flow of Carreau Liquid with Partial Slip and Newtonian Heating

S. Eswaramoorthi^{1*}, K. Loganathan³, S. Sivasankaran^{2**}, M. Bhuvanewari², S. Rajan³

¹Department of Mathematics, Dr. N. G. P. Arts and Science College, Coimbatore, India

²Department of Mathematics, King Abdulaziz University, Jeddah, Saudi Arabia

³Department of Mathematics, Erode Arts and Science College, Erode, India

*Corresponding author E-mail: ¹eswaran.bharathiar@gmail.com, ²sd.siva@yahoo.com

Abstract

This work deliberates the MHD flow of Carreau liquid past a stretching plate with thermal radiation, viscous dissipation and Joule heating. Additionally, partial velocity slip and Newtonian heating effects are included in our study. The similarity transformations are used to convert the governing dimensional partial differential equations into dimensionless ordinary differential equations. Homotopy analysis method (HAM) is employed to find the convergent series solutions of the governed non-linear ordinary differential equations. It is found that the magnetic field parameter slowdown the liquid motion and rises the liquid temperature. In addition, heat generation parameter enhances the thermal boundary layer thickness and chemical reaction parameter suppresses the solutal boundary layer thickness.

Keywords: Carreau liquid; Partial slip; Suction/injection; Newtonian heating; Chemical reaction.

1. Introduction

Due to its several industrial and engineering applications, many researchers are interested to study the boundary layer flow and heat transfer over a stretching plate. For example, polymer extrusion, wire drawing, glass fiber production, stretching of plastic films, etc. The problem of boundary layer flow and heat transfer over a stretching sheet was investigated by Rushi Kumar [1]. He found that the velocity boundary layer thickness enhances with raising the convective parameter. Few studies on boundary layer flow and heat transfer over a stretching sheet are [2]-[7].

The simplest generalized Newtonian fluid is the power-law model. But this model cannot predict the viscosity for very small or very large shear rates. Carreau fluid model overcome this restriction and valid for very small or very large shear rates. This model was initiated by Carreau [8] in 1972. In combustion chambers, propulsion devices for aircraft, nuclear plants and solar power technology, the impact of thermal radiation is more important. In this regard, many researchers are interested to study the thermal radiation effect in different fluids, see [9]-[14].

Motivations of the above studies, the present study is made on boundary layer flow and heat transfer of MHD mixed convective flow of Carreau liquid with thermal radiation, viscous dissipation, partial velocity slip and Newtonian heating in detail.

2. Mathematical Formulation:

We consider the 2D flow of a Carreau liquid past a stretching plate with velocity $U_w = ax, a > 0$. The x -axis is taken along the plate and y -axis is perpendicular of the plate. A constant magnetic field of strength B_0 is applied on the y direction and the fluid makes electrically conducted. We assume the plate temperature is

T_w and concentration is C_w which is always higher than the free stream temperature T_∞ and concentration C_∞ . In addition, the liquid phase is chemically reacted, heat generating or absorbing and viscous dissipated. The effect of Joule heating are retained. The heat transfer is happening with radiation and Newtonian heating. The boundary layer equations with the above assumptions are considered as follows [7],

$$\frac{\partial u_1}{\partial x} + \frac{\partial u_2}{\partial y} = 0, \quad (1)$$

$$u_1 \frac{\partial u_1}{\partial x} + u_2 \frac{\partial u_1}{\partial y} = \nu \frac{\partial^2 u_1}{\partial y^2} + \nu \frac{3(n-1)}{2} \lambda_1^2 \left(\frac{\partial u_1}{\partial y} \right)^2 \frac{\partial^2 u_1}{\partial y^2} - \frac{\sigma B_0^2}{\rho} u_1 \quad (2)$$

$$u_1 \frac{\partial T}{\partial x} + u_2 \frac{\partial T}{\partial y} = \alpha \left(1 + \frac{16\sigma^* T_\infty^3}{3kk^*} \right) \frac{\partial^2 T}{\partial y^2} + \frac{\nu}{c_p} \left(\frac{\partial u_1}{\partial y} \right)^2 + \frac{\sigma B_0^2}{\rho} u_1^2 + \frac{Q}{\rho c_p} (T - T_\infty) \quad (3)$$

$$u_1 \frac{\partial C}{\partial x} + u_2 \frac{\partial C}{\partial y} = D_B \frac{\partial^2 C}{\partial y^2} - k_0 (C - C_\infty) \quad (4)$$

where $u_1, u_2, \nu, n, \lambda_1, \sigma, \rho, T, \alpha, \sigma^*, k^*, c_p, Q, C, D_B,$ and k_0 are the x -direction velocity, y -direction velocity, kinematic viscosity, power law index, time constant, electrical conductivity, density, fluid temperature, thermal diffusivity, Stefan-Boltzmann constant, mean absorption coefficient, specific heat, internal heat generation (>0) or absorption (<0), concentration, mass diffusivity and the coefficient of chemical reaction, respectively.

The supporting boundary conditions are

$$u_1 = U_w = ax + L \frac{\partial u_1}{\partial y}, u_2 = V_w, \frac{\partial T}{\partial y} = -h_c T, C = C_w \text{ at } y = 0$$

$$u \rightarrow 0, \frac{\partial u}{\partial y} \rightarrow 0, T \rightarrow T_\infty, C \rightarrow C_\infty \text{ as } y \rightarrow \infty. \quad (5)$$

We use the following similarity variables for converting the dimensional boundary layer equation into dimensionless equations,

$$\eta = \sqrt{\frac{a}{v}}y, u_1 = axf'(\eta), u_2 = -\sqrt{av}f(\eta), \theta = \frac{T-T_\infty}{T_\infty}, \phi = \frac{C-C_\infty}{C_w-C_\infty} \tag{6}$$

The dimensionless form of the equations (2-4) are

$$f'''' + ff'' - f'^2 + \frac{3(n-1)}{2}We^2f''^2f''' - Mf' = 0, \tag{7}$$

$$\frac{1}{Pr} \left(1 + \frac{4}{3}Rd\right) \theta'' + f\theta' + Ec(f''^2 + Mf'^2) + Hg\theta = 0, \tag{8}$$

$$\frac{1}{Sc} \phi'' + f\phi' - Cr\phi = 0, \tag{9}$$

with the boundary conditions

$$f(0) = f_w, f'(0) = 1 + \lambda f''(0), f'(\infty) = 0, f''(\infty) = 0, \theta'(0) = -N[1 + \theta(0)], \theta(\infty) = 0, \phi'(0) = 1, \phi(\infty) = 0, \tag{10}$$

where $We^2 = \frac{a^3x^2\lambda_1^2}{v}$, $M = \frac{\sigma B_0^2}{\rho c}$, $Pr = \frac{\nu}{\alpha}$, $Rd = \frac{4\sigma^*T_\infty^3}{kk^*}$, $Ec = \frac{a^2x^2}{c_pT_\infty}$, $Hg = \frac{Q}{\rho a c_p}$, $Sc = \frac{\nu}{D_B}$, $Cr = \frac{k_0}{a}$, $f_w = -\frac{V_w}{\sqrt{av}}$, $\lambda = L\sqrt{\frac{a}{v}}$ and

$N = h_c\sqrt{\frac{v}{a}}$ are the Weissenberg number, magnetic field parameter, Prandtl number, thermal radiation parameter, Eckert number, internal heat generation/absorption parameter, Schmidt number, chemical reaction parameter, suction/injection parameter, slip parameter and thermal conjugate parameter, respectively.

Since the local Nusselt number and local Sherwood number are important physical parameters, they are defined as follows,

$$Nu/\sqrt{Re} = \left(1 + \frac{4}{3}Rd\right) \left(1 + \frac{1}{\theta(0)}\right) \text{ and } Sh/\sqrt{Re} = -\phi'(0).$$

HAM Solution:

The governing non-linear ordinary differential equations (7)-(9) with the boundary conditions (10) are solved using homotopy analysis method. The initial guesses of HAM solutions are $f_0(\eta) = f_w + \frac{1}{1+\lambda}(1 - Exp(-\eta))$, $\theta_0(\eta) = \frac{NExp(-\eta)}{1-N}$ and $\phi_0(\eta) = Exp(-\eta)$. These convergent series solution contains the auxiliary parameters h_f, h_θ and h_ϕ , and these parameters are adjust and control the HAM series solutions. The h_f, h_θ and h_ϕ curves are displayed in the Figure 1. It is concluded from this figure that the range values of $-1.4 \leq h_f \leq -0.1$, $-2.1 \leq h_\theta \leq -0.1$ and $-2 \leq h_\phi \leq -0.4$, respectively. It is observed that our HAM solutions convergence in the whole region of η when $h_f = h_\theta = h_\phi = -1$.

Result and Discussion:

In this section, we analyze the impact of various physical parameters on velocity, temperature and concentration profiles in graphical form with fixed values of Prandtl number ($Pr = 2$) and Schmidt number ($Sc = 2$). Table 1 presents the order of approximations of $-f''(0), -\theta'(0)$ and $-\phi'(0)$ which are necessary for a convergent of a solution. It is found that 15th order of approximation is enough for the velocity and temperature profiles and 20th order of approximation is sufficient for concentration profile. Table 2 shows the comparison of the local Nusselt number for different values of M, f_w, We, Cr and Sc values with Hayat et al. [7]. It is found that our results are in good agreement.

The impact of Weissenberg number, slip parameter, magnetic field and suction/injection on velocity profile is shown in Figures 2(a-d). It is seen that the momentum boundary layer thickness enhances with increasing the Weissenberg number and it reduces

with rising the slip parameter, magnetic field parameter and suction/injection parameter. The behavior of magnetic field parameter, Eckert number, heat generation/absorption parameter and thermal conjugate parameter on temperature profile is illustrated in Figures 3(a-d). We found that the temperature and thermal boundary layer thickness increase with enhancing the magnetic field parameter, Eckert number, heat generation/absorption parameter and thermal conjugate parameter. Effect of chemical reaction and suction/injection parameter on concentration profile is depicted in Figures 3(a-b) and found that the solutal boundary layer thickness reduces with enhancing the chemical reaction parameter and suction/injection parameter. The correlation equations of the local Nusselt number and local Sherwood number are

$$\frac{Nu}{\sqrt{Re}} = 1.20293 - 0.11176M + 0.00511\lambda + 0.00078n + 0.69513Rd - 0.26286Ec + 1.11787N$$

$$\frac{Sh}{\sqrt{Re}} = 1.66960 - 0.0434M - 0.03554\lambda + 0.000474n + 0.52537Cr$$

This equation is valid in the range of $0 \leq M \leq 1, 1 \leq \lambda \leq 3, 0 \leq n \leq 5, 0 \leq Rd \leq 0.5, 0 \leq Ec \leq 2, 0 \leq N \leq 0.6$ and $1 \leq Cr \leq 2$ with maximum error of 0.08.

3. Conclusions:

We investigate the partial slip and Newtonian heating on convective flow of a Carreau liquid past a stretching plate with magnetic field, Joule heating, suction/injection and heat generation/absorption. The momentum boundary layer thickness reduces on enhancing the magnetic field parameter and slip parameter and it rises by increasing the Weissenberg number. The thermal boundary layer thickness rises with increasing the magnetic field parameter, Eckert number, heat generation/absorption parameter and thermal conjugate parameter. The solutal boundary layer thickness drops with the chemical reaction and suction/injection parameters.

Table1: Order of approximation of $-f''(0), -\theta'(0)$ and $-\phi'(0)$.

Order	$-f''(0)$,	$-\theta'(0)$	$-\phi'(0)$
1	0.56063	0.77083	1.58333
5	0.55400	0.77540	2.10686
10	0.55395	0.77535	2.13821
15	0.55395	0.77536	2.13917
20	0.55395	0.77536	2.13920
25	0.55395	0.77536	2.13920
30	0.55395	0.77536	2.13920
35	0.55395	0.77536	2.13920
40	0.55395	0.77536	2.13920

Table2: Comparison of local Nusselt number for different values of M, f_w, We, Cr and Sc values with Hayat et al. [7].

M	f_w	We	Cr	Sc	Present Study	Hayat et al. [7]
0.0	0.5	0.2	1.0	1.0	1.46993	1.46992
0.36					1.46223	1.46224
0.64					1.45729	1.45730
0.04	0.0	0.2	1.0	1.0	1.17625	1.17625
	0.4				1.40679	1.40679
	0.6				1.53295	1.53289
0.04	0.5	0.0	1.0	1.0	1.46724	1.46722
		0.3			1.47083	1.47082
		0.6			1.47526	1.47525
0.04	0.5	0.2	0.0	1.0	0.93093	0.93093
			0.4		1.18575	1.18575
			0.8		1.38270	1.38271
0.04	0.5	0.2	1.0	0.9	1.37418	1.37416
				1.2	1.65053	1.65045
				1.4	1.82349	1.82764

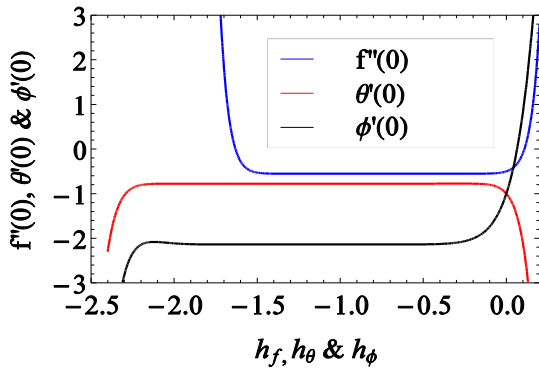


Figure 1: h curve of $f''(0)$, $\theta'(0)$ and $\phi'(0)$.

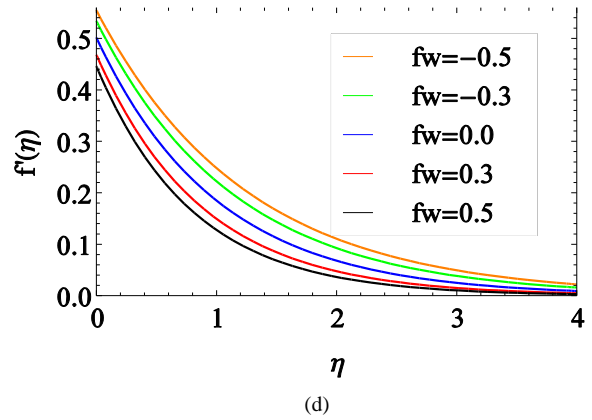
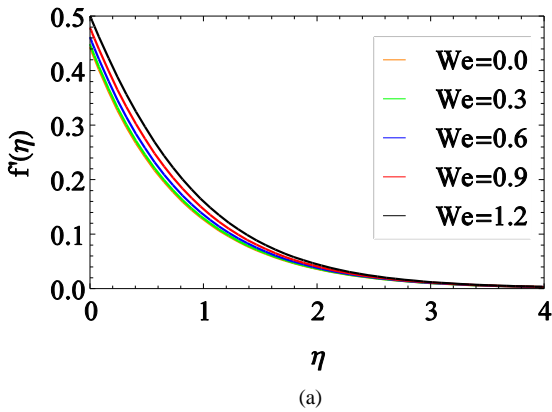
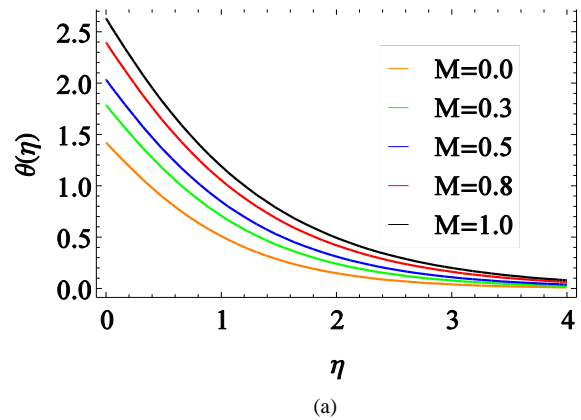


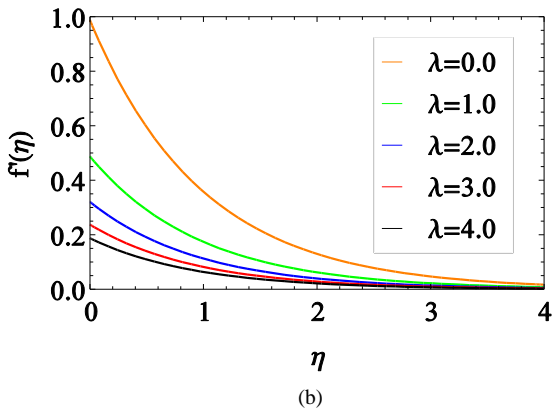
Figure 2: Velocity profile different values of Weissenberg number (a), slip parameter (b), magnetic field parameter (c) and suction/injection parameter (d).



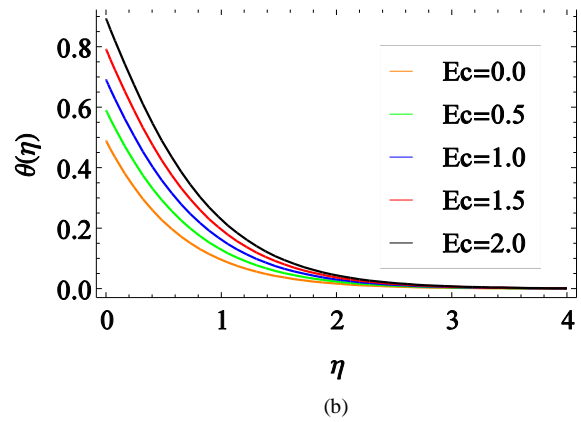
(a)



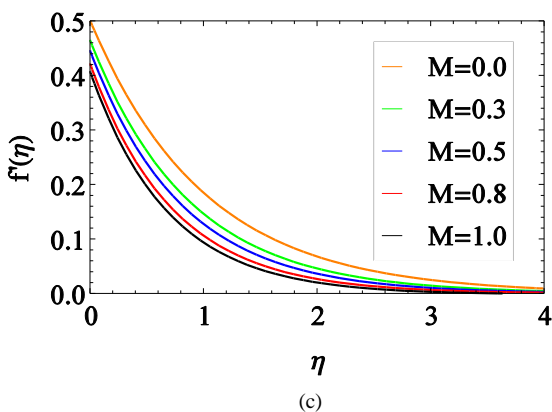
(a)



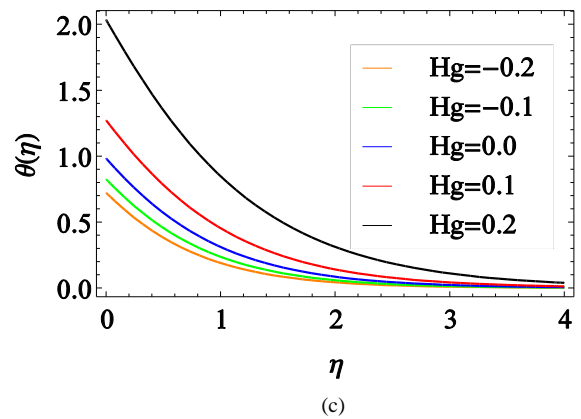
(b)



(b)



(c)



(c)

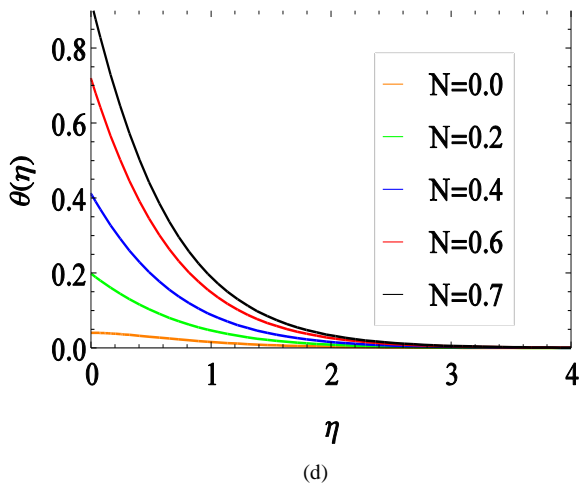


Figure 3: Temperature profile for different values of magnetic field parameter (a), Eckert number (b), heat generation/absorption parameter (c) and conjugate parameter (d).

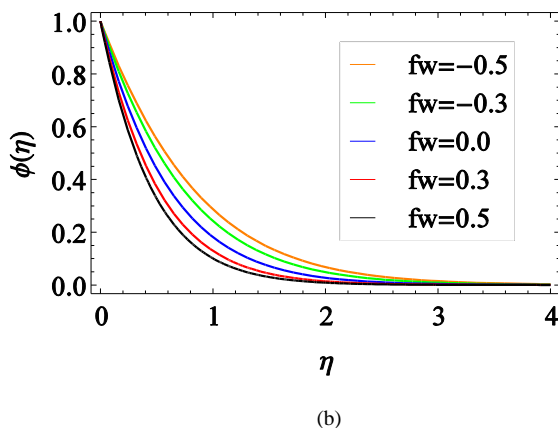
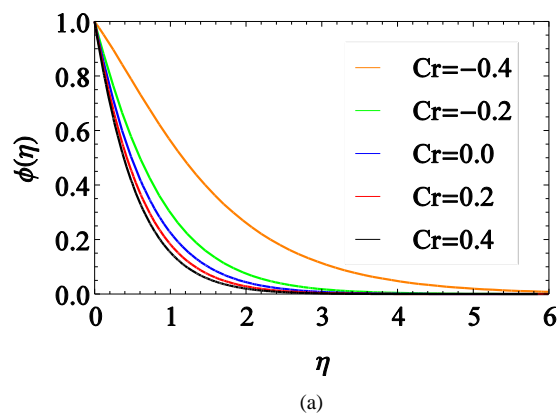


Figure 4: Concentration profile for different values of chemical reaction parameter (a) and suction/injection parameter (b).

References

- [1] Rushi Kumar B (2013), MHD boundary layer flow on heat and mass transfer over a stretching sheet with slip effect. *J. Naval Archi. Marine Engin.* 10, 16-26.
- [2] Olajuwon BI (2011), Convective heat and mass transfer in a hydromagnetic Carreau fluid past a vertical porous plated in presence of thermal radiation and thermal diffusion. *Therm. Sci.* 15, 241-252.
- [3] Rushi Kumar B & Gangadhar K (2012), Heat generation effects on MHD boundary layer flow of a moving vertical plate with suction. *J. Naval Archi. Marine Engin.* 9, 153-162.
- [4] Rushi Kumar B & Sivaraj R (2013), Heat and mass transfer in MHD viscoelastic fluid flow over a vertical cone and flat plate with variable viscosity. *Int. J. Heat Mass Transf.* 56, 370-379.

- [5] Sivaraj R & Rushi Kumar B (2013), Viscoelastic fluid flow over a moving vertical cone and flat plate with variable electric conductivity. *Int. J. Heat Mass Transf.* 61, 119-128.
- [6] Srinivas S, Reddy PBA & Prasad BSRV (2014), Effects of chemical reaction and thermal radiation on MHD flow over an inclined permeable stretching surface with non-uniform heat source/sink: An application to the dynamics of blood flow. *J. Mech. Med. Biol.* 14(5), 1-24.
- [7] Hayat T, Ullah I, Ahmad B & Alsaedi A (2017), Radiative flow of Carreau liquid in presence of Newtonian heating and chemical reaction. *Results Phys.* 7, 715-722.
- [8] Carreau PJ (1972), Rheological equations from molecular network theories. *Trans. Soc. Rheol.* 116, 99-127.
- [9] Srinivas S & Muthuraj R (2010), Effects of thermal radiation and space porosity on MHD mixed convection flow in a vertical channel using homotopy analysis method. *Comm. Nonlinear Sci. Numerical Simul.* 15(08), 2098-2108.
- [10] Eswaramoorthi S, Bhuvanewari M, Sivasankaran S & Rajan S (2015), Effect of radiation on MHD convective flow and heat transfer of a viscoelastic fluid over a stretching surface. *Procedia Eng.* 127, 916-923.
- [11] Eswaramoorthi S, Bhuvanewari M, Sivasankaran S & Rajan S (2016), Soret and Dufour effects on viscoelastic boundary layer flow, heat and mass transfer in a stretching surface with convective boundary condition in the presence of radiation and chemical reaction. *Scientia Iranica Transaction B, Mech. Engin.* 23(6), 2575-86.
- [12] Karthikeyan S, Bhuvanewari M, Sivasankaran S & Rajan S (2016), Soret and Dufour effects on MHD mixed convection heat and mass transfer of a stagnation point flow towards a vertical plate in a porous medium with chemical reaction, radiation and heat generation. *J. Appli. Fluid Mech.* 9(3), 1447-1455.
- [13] H. Niranjana, S. Sivasankaran & M. Bhuvanewari, Chemical reaction, Soret and Dufour effects on MHD mixed convection stagnation point flow with radiation and slip condition, *Scientia Iranica Transaction B, Mech. Engin.* 24(2), (2017) 698-706.
- [14] Sivasankaran S, Niranjana H & Bhuvanewari M (2017), Chemical reaction, radiation and slip effects on MHD mixed convection stagnation-point flow in a porous medium with convective boundary condition, *Int. J. Numeri. Methods Heat Fluid Flow* 27(2), 454-470.